Geophysical Research Letters

RESEARCH LETTER
10.1029/2020GL088998

Modeling Marsh-Forest Boundary Transgression in Response to Storms and Sea-Level Rise

J. Carr[1], G. Guntenspergen[1], and M. Kirwan[2]

[1]U.S. Geological Survey Patuxent Wildlife Research Center, Laurel, MD, USA, [2]Virginia Institute of Marine Science, College of William and Mary, Gloucester Point, VA, USA

Key Points:
- Upland transgression depends on the sequence of water-level deviations and slope
- Punctuated transgressive events drive the forest boundary upslope and inland
- With high sea-level rise rates, retreat rates tend to revert to a slope-sea-level rise-dominated process

Supporting Information:
- Supporting Information S1

Correspondence to:
J. Carr,
jcarr@usgs.gov

Citation:
Carr, J., Guntenspergen, G., & Kirwan, M. (2020). Modeling marsh-forest boundary transgression in response to storms and sea-level rise. *Geophysical Research Letters*, *47*, e2020GL088998. https://doi.org/10.1029/2020GL088998

Received 27 MAY 2020
Accepted 31 JUL 2020
Accepted article online 10 AUG 2020

Abstract The lateral extent and vertical stability of salt marshes experiencing rising sea levels depend on interacting drivers and feedbacks with potential for nonlinear behaviors. A two-dimensional transect model was developed to examine changes in marsh and upland forest lateral extent and to explore controls on marsh inland transgression. Model behavior demonstrates limited and abrupt forest retreat with long-term upland boundary migration rates controlled by slope, sea-level rise (SLR), high water events, and biotic-abiotic interactions. For low to moderate upland slopes the landward marsh edge is controlled by the interaction of these inundation events and forest recovery resulting in punctuated transgressive events. As SLR rates increase, the importance of the timing and frequency of water-level deviations diminishes, and migration rates revert back to a slope-SLR-dominated process.

1. Introduction

Understanding the response of salt marshes to rising sea levels is important, as they provide critical ecosystem services at the land-sea interface (Allen, 2000; Weinstein & Kreeger, 2007). Both lateral extent and vertical stability of salt marshes in response to rising sea levels have been shown to be functions of interacting drivers and feedbacks (Fagherazzi et al., 2012; FitzGerald & Hughes, 2019; Kirwan, Temmerman, et al., 2016), and the ecogeomorphic evolution of these systems can exhibit nonlinear behavior. For example, lateral salt marsh loss may provide inorganic sediment to the marsh platform (Hopkinson et al., 2018; Mariotti & Carr, 2014), allowing it to better maintain pace with SLR. SLR may also lead to marsh expansion through upland migration (Feagin et al., 2010; Kirwan, Walters, et al., 2016; Raabe & Stumpf, 2016; Schieder et al., 2017). If marshes cannot keep vertical pace with SLR, then landward migration is essential for their survival (Schuerch et al., 2018). Marsh migration into retreating uplands is spatially extensive and leads to reorganization of coastal ecosystems and economies (Gedan & Fernandez-Pascual, 2019, Fagherazzi, Anisfeld, et al., 2019; Langston et al., 2017; Kirwan & Gedan, 2019). While most conceptual and numerical models of marsh migration assume passive retreat of coastal forests (Doyle et al., 2010; Duran Vinent et al., 2019; Enwright et al., 2016; Kirwan, Temmerman, et al., 2016; Schuerch et al., 2018), the processes influencing the pace of ecosystem transgression are likely more complex and remain poorly understood (Fagherazzi, Anisfeld, et al., 2019; Kirwan & Gedan, 2019).

Marsh migration into retreating upland forests is considered to be primarily controlled by the local rate of SLR and the slope of adjacent uplands (Brinson et al., 1995; Kirwan, Temmerman, et al., 2016). However, the pace and mechanisms of ecosystem change are likely controlled by a more complex interplay between gradual SLR and episodic events (Fernandes et al., 2018; Fagherazzi, Anisfeld, et al., 2019; Fagherazzi, Nordio, et al., 2019; Schieder and Kirwan, 2019). Soils and herbaceous vegetation respond quickly (Anisfeld et al., 2017), but the extent of mature forests may lag behind SLR (Kirwan et al., 2007; Williams et al., 1999). However, tree seedlings are more sensitive to saltwater than adult trees, so regeneration ceases before adult mortality occurs (Kirwan et al., 2007; Williams et al., 1999). Although gradual SLR can lead to reduced tree growth rates (Robichaud & Bégin, 1997) with eventual senescence, episodic disturbance events such as storms and fires may be required to initiate ecosystem replacement. These observations inspire the application of punctuated equilibrium concepts to the transgression of coastal ecosystems, where episodic storms superimposed on gradual SLR set the pace and extent of marsh migration into forests (Clark, 1986; Fagherazzi, Anisfeld, et al., 2019; Kearney et al., 2019; Kirwan & Gedan, 2019; Kirwan et al., 2007; Schieder & Kirwan, 2019; Williams et al., 1999; Young, 1995). We present a two-dimensional transect model developed to explore the interplay of stochastic drivers and biotic-abiotic feedbacks affecting changes in

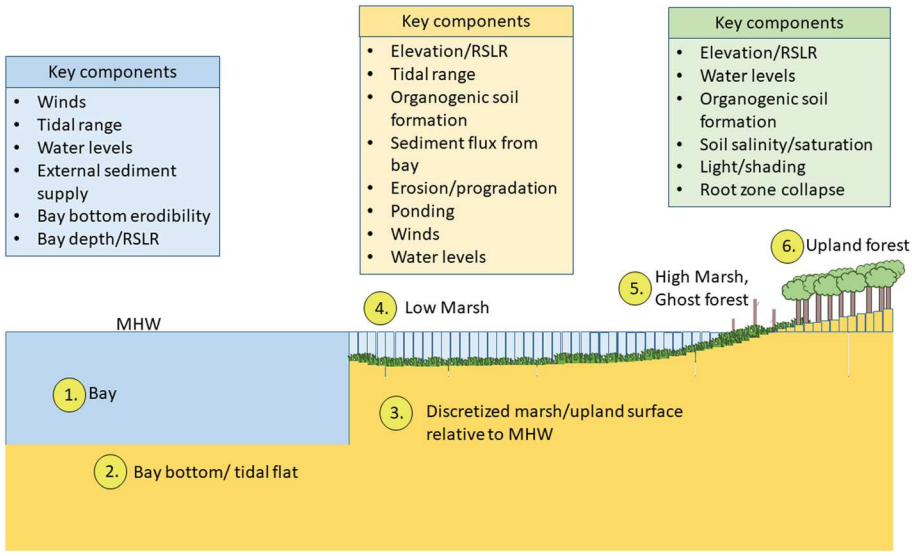

Figure 1. Schematic of the key components of the marsh transgression model from the bay (1) to the upland forest (6).

marsh lateral extent, vertical stability, and the potential for forest retreat and marsh transgression inland. The model was used to explore how different system characteristics (tidal characteristics, SLR, forest recovery, and root zone collapse) may affect marsh transgression and forest retreat.

2. Methods

2.1. Model Overview

The model encompasses an idealized back barrier bay coupled to a collection of ~1-m-wide discretized cells extending from bay-marsh edge to upland forested regions (Figure 1). Inundation frequency is determined by the elevation of the individual cells, stochastic water levels, and tides and is affected by mineral deposition (section 2.2) and organogenic soil formation rates (section 2.5). Wind- and water-level data from three sites in the mid-Atlantic Coast of the United States were used to generate seasonal auto and cross-correlated hourly synthetic stochastic winds and water levels (section 2.3). The model incorporates feedbacks between fetch, wave growth, and lateral marsh erosion and sediment supply to the marsh platform. Vegetation at each cell along the transect was modeled with six distinct states: grass/saltmarsh, tree seedlings, tree saplings, trees, dead standing trees, and bare soil (section 2.4) with transition between states based on a transition matrix depending on both inundation history and the prior vegetation state, allowing for positive and negative feedbacks among different vegetation states and environmental drivers. This forest-marsh model allowed for exploring differences in forest retreat rates and the dynamics of the marsh coastal forest boundary under varied rates of SLR, upland slope, wind, and water-level statistics.

2.2. Transect Model

The transect model builds upon a simple coupled model (Kirwan, Walters, et al., 2016; Mariotti & Carr, 2014), where an idealized mainland back barrier marsh is coupled to an adjacent tidal flat that is conceptually connected to some external body of water (tidal channel/tidal inlet) which acts as a source of allochthonous sediment. The model conserves fluid volume between N conceptual boxes (Figure 1). These fluid boxes are defined completely by depth, h_n, and width, w_n, of element n relative to mean high water (MHW). Changes in (1) the depth due to vertical erosion and deposition and (2) the width of an element due to wind wave lateral erosion and bank creep affect both the depth and width of laterally adjacent elements. Changes in the depth of each fluid element with time are computed as

$$\frac{dh_n}{dt} = -F_n/\rho_s + R - O_n/\rho_o, \tag{1}$$

where F_n ($\mathrm{ML^{-2}\ T^{-1}}$) is the sediment flux exchanged with other elements, O_n ($\mathrm{ML^{-2}\ T^{-1}}$) is the organogenic sediment production, computed as function of the standing vegetation, R ($\mathrm{LT^{-1}}$) is relative SLR, and $\rho_s = 1{,}000\ \mathrm{kg\ m^{-3}}$ and $\rho_o = 300\ \mathrm{kg\ m^{-3}}$ are mineral sediment bulk density and organic bulk density,

respectively (Mariotti & Carr, 2014). The mineral sediment flux is calculated based on a local sediment concentration C_n and settling velocity $w_{s,marsh}$ as $F_n = C_n f_{ind.} w_{s,marsh}$ and the flood fraction of time the element is inundated $f_{ind.}$. Sediment flux to the marsh platform is assumed to predominantly originate from the tidal flat, with some supply from ponds which can form internal to the marsh platform. Sediment resuspension is assumed to be zero when an element is vegetated accounting for the significant wind wave dissipation and subsequent reduction in near bed shear stresses. Lateral and vertical changes are coupled via conservation of fluid volume among adjacent elements,

$$\frac{d\left(\sum_{j=n-1}^{n+1} h_j w_j\right)}{dt} = 0. \tag{2}$$

Deviations from conservation arise from allochthonous sediment supply, organogenic soil formation, and SLR (Mariotti & Carr, 2014). Details of the sediment resuspension and redistribution across the transect can be found in supporting information (Text S1).

2.3. Winds and Deviations in Water Levels as a Seasonal Drivers

Hourly offshore wind records (1984 to 2016) from station CHVL2 (Mccall, 2007) were rescaled to 10 m aloft values assuming a fully rough sea surface. Synthetic wind speed time series were generated from a fourth-order Markov chain Monte Carlo approach (Karatepe & Corscadden, 2013) using monthly transitions matrices accounting for autocorrelation and seasonality in the hourly wind speed and direction records. Hourly water-level predictions and measurements for three tide stations (Mccall, 2007, Figure S1), from 1984 through 2015 for Wachapreague, VA (tide range 1.225 m), and Kiptopeke, VA (tide range 0.793 m), and 2005 through 2015 for Bishops Head, MD (tide range 0.536 m), were used to acquire deviations from the predicted tides (Figure S2). Locations were chosen to cover a range of tidal characteristics relatively close to the record of offshore winds. Transition probability matrices for each site water-level deviations were based on (1) water-level deviations of the prior 3 hr and (2) longitudinal wind speed at a site-specific lag that reproduced similar cross-correlation to the records (Figure S3). A single synthetic time series of wind speed and direction thus allowed for generation of site-specific synthetic water-level deviations for three different tidal characteristics (Figures S4–S6) which were then combined with synthetic tides generated using the TideHarmonic package in R based on individual site tidal harmonics (Figure S7).

2.4. Forest-Marsh Model

The vegetation model considers six distinct states, herbaceous/saltmarsh (G), seedling (S_e), sapling (S_a), tree (T), dead standing tree (D), and bare (B) with the transition matrix depending on the vegetation states of an element comprised of transition probabilities of establishment (G_{est}, $S_{e,est}$), aging ($S_{e,age}$, $S_{a,age}$) and mortality (G_{mort}, $S_{e,mort}$, T_{mort}). Thus, for element n at time i, G_i is the fraction of the element covered by herbaceous vegetation ranging from 0 to a carrying capacity term, G_{cc}. In simplest form,

$$\begin{bmatrix} G_i \\ S_{e,i} \\ S_{a,i} \\ T_i \\ D_i \\ B_i \end{bmatrix} = V_i \text{ is the column matrix of vegetation states, and} \tag{3}$$

$$M_i = \begin{bmatrix} 1-G_{mort} & 0 & 0 & 0 & 0 & G_{est} \\ 0 & 1-S_{e,mort}-S_{e,age} & 0 & 0 & 0 & S_{e,est} \\ 0 & S_{e,age} & 1-S_{a,mort}-S_{a,age} & 0 & 0 & 0 \\ 0 & 0 & S_{a,age} & 1-T_{mort} & 0 & 0 \\ 0 & 0 & S_{a,mort} & T_{mort} & 1-D_{fall} & 0 \\ G_{mort} & S_{e,mort} & 0 & 0 & D_{fall} & 1-S_{e,est}-G_{est} \end{bmatrix}$$

is the transition matrix at time i for element n, then

$$M_i V_i = V_{i+1}$$

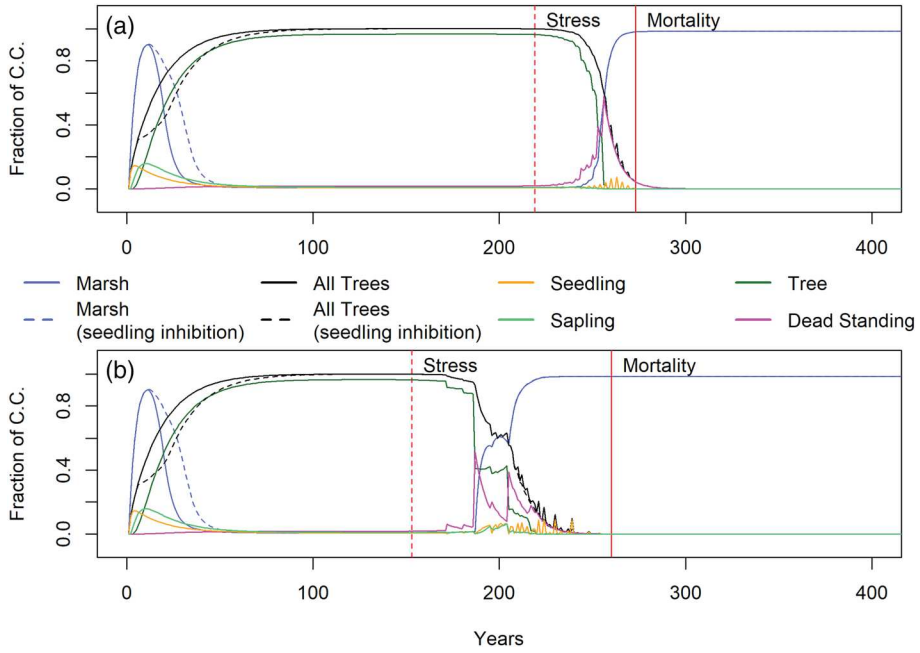

Figure 2. Forest-marsh model behavior for an initially bare surface situated 1 m above MHW experiencing a SLR rate or 4 mm/yr under (a) harmonic tides and (b) the same harmonic tides with wind modified water levels. All lines are relative to the herbaceous or forest carrying capacities (C.C.). Vertical lines indicate the onset of saline inundation stress conditions and when the inundation is enough to force full forest mortality and the inability to regrow.

The transition matrix captures feedback mechanisms across the marsh-tree boundary. At the two end-member stable vegetated states (herbaceous and forested), a carrying capacity, in terms of biomass, or fractional cover can be expected. Here we use fractional cover at the surface (m^2/m^2) based on stem area/basal area estimates with $T_{cc} = 0.0048$, or 48 m^2 ha^{-1} (Jokela et al., 2004) and $G_{cc} = 0.0048$ m^2/m^2, assuming 1.95 mm radius stem with a maximum stem density of 400 shoot/m^2 (Valiela et al., 1978).

In the absence of inundation, a herbaceous landscape is expected to transition to a forested landscape via seedling establishment and aging with herbaceous vegetation either facilitating seedling establishment by lowering the water table via evapotranspiration (Poulter et al., 2009) or inhibiting pine seedling establishment due to increasing soil salinity (Kurz & Wagner, 1957). Once a forest has established, light conditions become unfavorable for herbaceous vegetation. On top of these feedbacks, saturated soil conditions both reduce soil respiration rates and, depending on duration of saturation, increase seedling (Kirwan et al., 2007; Poulter et al., 2009), sapling, and tree mortality rates (Williams et al., 1999) (Figure 2).

These mechanisms are incorporated into the transition probabilities by a set of logistic curves which model (1) saline water inundation impacts on seedlings $f_s(I)$, saplings and adult trees $f(I)$, (2) grass inhibition of seedlings $f(G)$, and (3) tree inhibition of herbaceous vegetation by shading $f(T)$ (Text S2).

The model behavior is not sensitive to carrying capacity terms, just the transition probabilities and logistic curves parameters and allows for modeling forest recovery rates to inundation events and the potential inhibition of seedling establishment (Figure 2). To illustrate general forest-marsh model behavior, we first conducted a simple experiment in which an initially bare piece of land situated 1 m above MHW experienced a SLR rate of 4 mm/yr. Full inundation of the land would occur by the end of a 400-year-long harmonic-derived tidal sequence (Figure 2a) or that same tidal sequence including wind-driven water-level deviations (Figure 2b). In both scenarios, initial establishment of herbaceous vegetation is lost to a developing forest with subsequent transition back to herbaceous vegetation due to saline inundation stress. The onset of saline stress conditions occurs approximately 50 years earlier when including wind-driven water-level deviations. Model parameters are explained in supporting information (Text S2, Table S2, Figures S9–S11).

2.5. Organogenic Soil Formation

Organic soil production in Equation 1 is coupled to the vegetation states in the forest-marsh model as

$$O_n = O_{marsh}(I)\frac{G_n}{G_{cc}} + O_{Tree}\frac{T_n}{T_{cc}} - R_{coll}\frac{D_n}{T_{cc}} \quad (4)$$

where marsh vegetation contribution $O_{marsh}(I)$ is a function of inundation, O_{tree} is a constant small accumulation given the presence of trees and a root zone collapse term, R_{coll}, due to the decomposition from the dead tree root mass. The contribution of marsh vegetation to organic matter is based on the approach of Mariotti and Carr (2014), where production is a quadratic function of depth from MHW to a maximum vegetation depth $D_{max} = 0.737(2r) - 0.092 + \text{MHW}$, determined by tidal range r (McKee & Patrick, 1988). This formulation represents marshes composed of *Schoenoplectus americanus* (Kirwan & Guntenspergen, 2015) and/or *Spartina alterniflora* (Morris et al., 2002). This depth-dependent quadratic relationship is transferred to be a function of inundation by using the average fraction of time each depth is inundated for a 300-year-long sequence of tides. The soil elevation contribution by the forest is assumed to be some minimal but non-zero amount, here set to 0.25 mm/yr and is dependent on the presence of trees. The last term, R_{coll}, represents the potential for root zone collapse to lower elevation when dead tree root biomass is present. This behavior is noted in mangroves (Cahoon et al., 2003) and incorporated into respiration-based elevation change models for Everglades tree islands (D'Odorico et al., 2011). However, rates in coastal forests are not yet constrained, and our model results are generated both including and neglecting this term to explore the potential impacts of root zone collapse.

2.6. Model Implementation

The element volume model was run at a tidal cycle time step with tidal cycle averaged wind wave characteristics and sediment redistribution characteristics. The number of elements in the model is dynamic. Adjacent elements are only combined if their elevation falls below the salt marsh vegetation limit, forming an internal pond with unique fetch, depth, and wind-wave characteristics, or if the element width shrinks below 0.75 m. Upland elements are added at a prescribed slope as the model surface is sinking due to SLR. The forest-marsh model was run annually based on the prior years' inundation frequency and vegetation states along the transect with the upland marsh edge and seaward forest edge, here defined by $G_{edge} = 0.1G_{cc}$ and $T_{edge} = 0.9T_{cc}$, respectively, tracked over time to examine forest retreat and marsh migration rates. Initial marsh platform and associated vegetation were generated from site-specific drivers (section 2.3) and an initial surface slope extending from the maximum marsh depth to 3.5 m above MHW. The marsh platform was then allowed to build for 300 years under 90 mg/L external sediment loading and a SLR rate of 1.5 mm/yr from an initial tidal flat width of 5 km to generate initial transect configurations (Figure S8). To provide a common fetch starting point, these marsh to upland initial configurations were then coupled to a new initial flat width (5 km). The tidal flat depth was then adjusted such that the boundary condition dispersive sediment flux equaled zero for the 85th percentile wind speed of the stochastic sequence of drivers to start close to the tidal flat depth-width manifold (Mariotti & Carr, 2014). The model was run for three different sequences of winds and corresponding synthetic water levels for the three different sites. These slope values correspond to SLR rates of 3,6, 9, and 12 mm/yr, upland slopes of 0.001, 0.005, and 0.01 covering a range of observed SLR (Ezer & Corlett, 2012), and upland slopes for the Chesapeake Bay and other coastal plains (0.001) and formerly glaciated continental margins such as the Plum Island Estuary (0.01) (Kirwan, Walters, et al., 2016).

3. Results

Expected forest retreat and consequent marsh migration can be estimated by (SLR-O_{tree})/slope. A forest on a low upland slope of 0.001 experiencing a SLR of 3 mm/yr provides an expected retreat rate of 2.75 m/yr with marsh migrating at the same pace. Over 100 years, the forest will have retreated, and the marsh migrated, 275 m upslope. A forest marsh boundary on a steeper sloped upland (0.01) experiencing the same SLR will have only retreated/migrated 27.5 m. In this manner, the lateral impact of any vertical deviation in water-level diminishes as slope increases and the gradient in inundation frequency is compacted laterally.

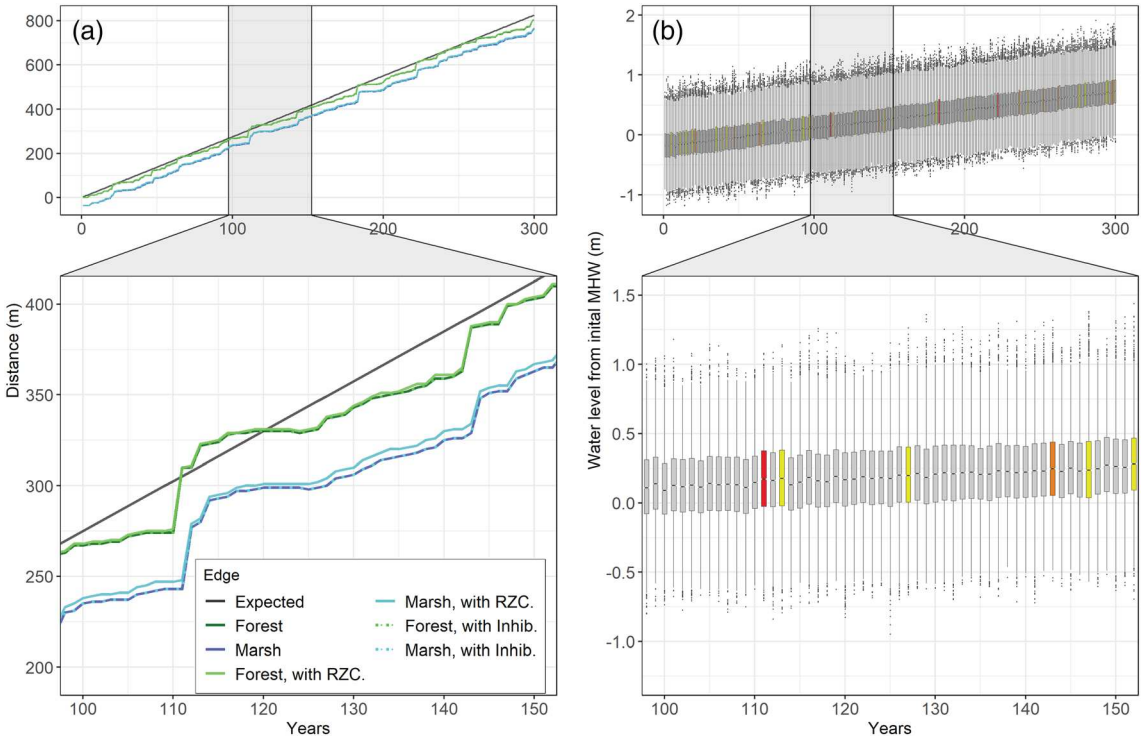

Figure 3. (a) Forest edge retreat and marsh edge migration for a slope of 0.001 and SLR of 3 mm/yr for one synthetic driver sequence derived from water levels measured at Bishops Head, MD both without and with root zone collapse (RZC) and seedling inhibition in comparison to the expected migration rate. Seedling inhibition has very little to no impact on the behavior of the forest and marsh boundaries whereas root zone collapse pushes the marsh edge further inland. (b) Boxplots showing the yearly water level distributions and the increase in water levels relative to initial MHW with years highlighted when the forest retreat rate exceeds twice (yellow), five times (orange), and 10 times (red) the expected retreat rate, respectively.

Setting the initial location of the forest boundary to zero, the forest edge progresses inland and upslope, sometimes smoothly, and sometimes in distinct jumps (Figure 3a) with the overall distance transgressed predominantly determined by slope and SLR. Unsurprisingly, the forest edge is not strongly affected by root zone collapse or seedling inhibition processes (Figure 3a) as modeled recovery rates are generally greater (>60 years) than the return of subsequent inundations. The marsh edge in contrast is maintained slightly further upland and inland by lowered elevations from root zone collapse (Figure 3a) with seedling inhibition having little effect on either edge. Discrepancies arising between the forest and marsh edges from these processes are temporarily erased from the system by the next large inundation event (Figure 3a). Accounting for water-level deviations, modeled long-term rates of marsh migration and forest retreat (estimated by linear regression) are similar (Tables 1 and S3), though the short-term transgression behaviors of these two edges differ (Figures 3a and S12).

The lateral distance the marsh boundary can migrate inland decreases with increasing slope; however, increasing SLR decreases the impact of water-level deviations on the overall migration rate (Table 1). This decreasing impact is consistent across different model runs for a given site, as well as across sites. Modeled migration rates overall tend to be lower than expected rates (Table 1) and more so for sites with higher variability in water-level deviations as the forest and marsh edges are responding to events near the extremes of the inundation distributions. As such, being at an elevation where inundation is possible does not imply inundation occurs, or that it occurs often enough consistently to push the forest back.

4. Discussion

Landscape models and simple topographic projections of ecosystem change typically assume that marshes replace forests when and where SLR exceeds a threshold elevation (Borchert et al., 2018; Enwright et al., 2016; Feagin et al., 2010; Kirwan, Walters, et al., 2016; Schile et al., 2014; Schuerch et al., 2013). While this static

Table 1
Linear Regression Determined Average Forest Retreat Rates (m/yr) Across Three 300 Year Sequences of Winds and Water-Level Deviations and the Percent Deviation From the Expected Rate of Migration for Each Prescribed Slope and SLR

	Slope SLR	3 (mm/yr)	Deviation	6 (mm/yr)	Deviation	9 (mm/yr)	Deviation	12 (mm/yr)	Deviation
Expect.	0.001	2.75	—	5.75	—	8.75	—	11.75	—
	0.005	0.55	—	1.15	—	1.75	—	2.35	—
	0.01	0.275	—	0.575	—	0.875	—	1.175	—
Bish.	0.001	2.73	−0.87%	5.72	−0.47%	8.72	−0.32%	11.73	−0.21%
	0.005	0.55	−0.89%	1.14	−0.54%	1.74	−0.34%	2.35	−0.21%
	0.01	0.27	−0.80%	0.57	−0.43%	0.87	−0.27%	1.17	−0.22%
Kipt.	0.001	2.71	−1.45%	5.71	−0.74%	8.71	−0.46%	11.71	−0.37%
	0.005	0.54	−1.44%	1.14	−0.73%	1.74	−0.69%	2.34	−0.32%
	0.01	0.27	−1.52%	0.57	−0.75%	0.87	−0.44%	1.17	−0.61%
Wach.	0.001	2.72	−0.92%	5.72	−0.50%	8.72	−0.31%	11.72	−0.22%
	0.005	0.55	−0.90%	1.14	−0.47%	1.74	−0.31%	2.35	−0.21%
	0.01	0.27	−0.90%	0.57	−0.49%	0.87	−0.33%	1.17	−0.23%

approach may be appropriate over large spatial and long temporal scales (Schieder & Kirwan, 2019), our modeling suggests that event-driven water-level fluctuations are critical drivers of transgression over decadal-century time scales. This more complex interplay leads to significant deviations from migration rates determined from simple SLR driven inundation of topography (Figures 3, S10, and S11). These model results are consistent with lateral forest retreat rates inferred from sediment cores and historical photographs that are only roughly correlated with the slope of adjacent uplands (Schieder et al., 2017; Schieder & Kirwan, 2019), which we suggest is due to deviations due to dynamic water-level fluctuations combined with the differential response of marsh and forest to those fluctuations.

Our results indicate that upland transgression depends on the sequence of water-level deviations, where punctuated transgressive events (Young, 1995) drive the forest boundary upslope and inland as in the conceptual ecological ratchet model (Kearney et al., 2019). These results are consistent with field observations that emphasize the role episodic storms play in determining the retreat of mature forests (Clark, 1986; Fagherazzi, Ansifeld, et al., 2019; Kearney et al., 2019; Kirwan et al., 2007; Kirwan & Gedan, 2019; Schieder & Kirwan, 2019; Williams et al., 1999; Young, 1995). Our model suggests that the impact of seedling inhibition, slower forest recovery, and root zone collapse all have little impact on the overall long-term migration rate of the forest and marsh edges. However, these processes do have an impact on the both yearly extent of the marsh (Figure 3) and distribution of marsh migration and forest retreat rates (Figure S10). Nevertheless, the lateral extent of transgressive events decreases with increasing slope, with broadly consistent deviations from an expected SLR slope-dependent migration (Tables 1 and S3). As SLR rates increase, the relative influence of water deviations diminish, periods of forest recovery (low water periods, or lack of inundation) decrease, and deviations from the expected migration rate decrease.

Observations of marsh migration and forest retreat are typically made by comparing a small number of historical maps or photographs through time (Raabe & Stumpf, 2016; Schieder et al., 2017; Smith, 2013). Our model results indicate that such an approach may be unable to properly isolate the influence of sea level rise on migration rates because it would be sensitive to the timing of water level fluctuations and episodic retreat/recovery. Migration rates extracted from two temporal points in the model provide insight into the time between measurements necessary for field or image-based measurements to accurately assess the long-term migration rate (Figure S11). Significant over or underestimation occurs for time periods less than a century with errors decreasing with increasing SLR. This suggests that trying to ascertain rates of migration from historic records may be troublesome unless the records cover significant periods of time (e.g., last 150 years, Raabe & Stumpf, 2016; Schieder et al., 2017) or the SLR rate over the period in question is high and relatively constant. Prediction of near-term migration rates is similarly troublesome as errors can be quite large (Table S4). This indicates that projections of marsh extent without accounting for water-level deviations and solely relying on slope/topography-SLR relationships are likely accurate only at long time

scales. However, these time scales are long enough for significant changes in the climate conditions including changes to both SLR, tidal characteristics, and storms to which these migration rates appear to be sensitive. Schieder and Kirwan (2019) noted that retreat was punctuated along individual transects (as in our transect model) but largely continuous when averaged over multi-km spatial scales. Dependence on time scale is therefore likely analogous to dependence on spatial scale when attempting to assess overall migration rates.

The transect model presented here has several limitations. Synthetic drivers are constrained to relatively short historical records and the formulation for stochastic drivers limits both wind- and water-level characteristics to short, assumed stationary, distributions. In reality, water-level deviations, tidal signals, and storms are shifting due to climate change impacts. The model neglects any rainfall impacts on inundation frequency and soil salinity. Local ground water dynamics may allow for freshwater connection to regional groundwater supplies (Williams et al., 1999, 2003) potentially allowing for non-halophytic vegetation to survive saline inundation events. Moreover, as an initial exploration of how multiple processes influence the migration of coastal ecosystems, the model depends on several poorly constrained parameters such as well-constrained species-specific inundation, salinity, and light tolerances. Further field-based studies are needed to improve our collective understanding of the key processes and parameters affecting both forest retreat and marsh migration. Despite these potential limitations, our model results lead to important qualitative insights that are consistent with field observations. For example, model results illustrate interactions between stochastic water-level events and long-term SLR that are consistent with concepts of punctuated equilibrium in extremely low relief coastal forests (e.g., Kearney et al., 2019; Young, 1995). Previous work noted deviations between SLR and forest retreat rates on decadal time scales, even though forest retreat accelerated in parallel with century-scale SLR (Schieder and Kirwan, 2019). Our model results offer a mechanistic explanation for these observations and uniquely suggest that deviations in migration rates induced by stochastic water-level fluctuations decrease with increasing slope, SLR, and time scale.

5. Conclusions

Marsh upland migration and forest retreat has been broadly thought of as being controlled by slope and SLR. In contrast, our model experiments suggest that the upland boundary migration rates are strongly controlled by stochastic water-level statistics and forest recovery times. This punctuated behavior is exhibited by the large marsh expansion due to high water events, with potential slow loss of high marsh due to forest recovery and conversion of high marsh to low marsh. Thus, in contrast to the relatively steady erosion of the seaward marsh edge, or a steady slope-dependent landward migration of the low marsh high marsh boundary, the landward upland marsh edge is predominantly controlled by the timing and frequency of extreme events. However, as SLR rates increase, the impact of stochastic water levels diminishes, and transgression rates revert to those predicted by surface slope and SLR.

Data Availability Statement

All data leveraged in this manuscript are available at www.ndbc.noaa.gov and https://doi.org/10.5066/P9XQ27F5.

Acknowledgments
This work was supported by USGS Land Change Science Climate R&D Program and Ecosystems Program and NSF grant DEB-1832221 to the Virginia Coast Reserve Long Term Ecological Research project. Any use of trade, product, or firm names is for descriptive purposes only and does not imply endorsement by the U.S. Government.

References

Allen, J. R. L. (2000). Morphodynamics of Holocene salt marshes: A review sketch from the Atlantic and southern North Sea coasts of Europe. *Quaternary Science Reviews*, *19*(12), 1155–1231. https://doi.org/10.1016/S0277-3791(99)00034-7

Anisfeld, S. C., Cooper, K. R., & Kemp, A. C. (2017). Upslope development of a tidal marsh as a function of upland land use. *Global Change Biology*, *23*(2), 755–766. https://doi.org/10.1111/gcb.13398

Borchert, S. M., Osland, M. J., Enwright, N. M., & Griffith, K. T. (2018). Coastal wetland adaptation to sea level rise: Quantifying potential for landward migration and coastal squeeze. *Journal of Applied Ecology*, *55*(6), 2876–2887. https://doi.org/10.1111/1365-2664.13169

Brinson, M. M., Christian, R. R., & Blum, L. K. (1995). Multiple states in the sea-level induced transition from terrestrial forest to estuary. *Estuaries*, *18*(4), 648–659. https://doi.org/10.2307/1352383

Cahoon, D. R., Hensel, P., Rybczyk, J., McKee, K. L., Proffitt, C. E., & Perez, B. C. (2003). Mass tree mortality leads to mangrove peat collapse at Bay Islands, Honduras after Hurricane Mitch. *Journal of Ecology*, *91*(6), 1093–1105. https://doi.org/10.1046/j.1365-2745.2003.00841.x

Clark, J. S. (1986). Coastal forest tree populations in a changing environment, southeastern Long Island, New York. *Ecological Monographs*, *56*(3), 259–277. https://doi.org/10.2307/2937077

D'Odorico, P., Engel, V., Carr, J. A., Oberbauer, S. F., Ross, M. S., & Sah, J. P. (2011). Tree–grass coexistence in the everglades freshwater system. *Ecosystems*, *14*(2), 298–310. https://doi.org/10.1007/s10021-011-9412-3

Doyle, T. W., Krauss, K., Conner, W., & Sang, A. (2010). Predicting the retreat and migration of tidal forests along the northern Gulf of Mexico under sea-level rise. *Forest Ecology and Management*, *259*(4), 770–777. https://doi.org/10.1016/j.foreco.2009.10.023

Duran Vinent, O., Johnston, R. J., Kirwan, M. L., Leroux, A. D., & Martin, V. L. (2019). Coastal dynamics and adaptation to uncertain sea level rise: Optimal portfolios for salt marsh migration. *Journal of Environmental Economics and Management*, *98*, 102262. https://doi.org/10.1016/j.jeem.2019.102262

Enwright, N. M., Griffith, K. T., & Osland, M. J. (2016). Barriers to and opportunities for landward migration of coastal wetlands with sea-level rise. *Frontiers in Ecology and the Environment*, *14*(6), 307–316. https://doi.org/10.1002/fee.1282

Ezer, T., & Corlett, W. (2012). Is sea level rise accelerating in the Chesapeake Bay? A demonstration of a novel new approach for analyzing sea level data. *Geophysical Research Letters*, *39*, L19605. https://doi.org/10.1029/2012GL053435

Fagherazzi, S., Anisfeld, S. C., Blum, L. K., Long, E. V., Feagin, R. A., Fernandes, A., et al. (2019). Sea level rise and the dynamics of the marsh-upland boundary. *Frontiers in Environmental Science*, *7*, 25. https://doi.org/10.3389/fenvs.2019.00025

Fagherazzi, S., Kirwan, M. L., Mudd, S. M., Guntenspergen, G. R., Temmerman, S., D'Alpaos, A., et al. (2012). Numerical models of salt marsh evolution: Ecological, geomorphic, and climatic factors. *Reviews of Geophysics*, *50*, RG1002. https://doi.org/10.1029/2011RG000359

Fagherazzi, S., Nordio, G., Munz, K., Catucci, D., & Kearney, W. S. (2019). Variations in persistence and regenerative zones in coastal forests triggered by sea level rise and storms. *Remote Sensing*, *11*(17), 2019. https://doi.org/10.3390/rs11172019

Feagin, R., Martinez, M., Mendoza-Gonzalez, G., & Costanza, R. (2010). Salt marsh zonal migration and ecosystem service change in response to global sea level rise: A case study from an urban region. *Ecology and Society*, *15*(4), 14. http://archives.pdx.edu/ds/psu/8706

Fernandes, A., Rollinson, C. R., Kearney, W. S., Dietze, M. C., & Fagherazzi, S. (2018). Declining radial growth response of coastal forests to hurricanes and nor'easters. *Journal of Geophysical Research: Biogeosciences*, *123*, 832–849. https://doi.org/10.1002/2017JG004125

FitzGerald, D. M., & Hughes, Z. (2019). Marsh processes and their response to climate change and sea-level rise. *Annual Review of Earth and Planetary Sciences*, *47*(1), 481–517. https://doi.org/10.1146/annurev-earth-082517-010255

Gedan, K. B., & Fernandez-Pascual, E. (2019). Salt marsh migration into salinized agricultural fields: A novel assembly of plant communities. *Journal of Vegetation Science*, *30*(5), 1007–1016. https://doi.org/10.1111/jvs.12774

Hopkinson, C. S., Morris, J. T., Fagherazzi, S., Wollheim, W. M., & Raymond, P. A. (2018). Lateral marsh edge erosion as a source of sediments for vertical marsh accretion. *Journal of Geophysical Research: Biogeosciences*, *123*, 2444–2465. https://doi.org/10.1029/2017JG004358

Jokela, E. J., Dougherty, P. M., & Martin, T. A. (2004). Production dynamics of intensively managed loblolly pine stands in the southern United States: A synthesis of seven long-term experiments. *Forest Ecology and Management*, *192*(1), 117–130. https://doi.org/10.1016/J.FORECO.2004.01.007

Karatepe, S., & Corscadden, K. (2013). Wind speed estimation: Incorporating seasonal data using markov chain models. *ISRN Renewable Energy*, *2013*, 1–9. https://doi.org/10.1155/2013/657437

Kearney, W. S., Fernandes, A., & Fagherazzi, S. (2019). Sea-level rise and storm surges structure coastal forests into persistence and regeneration niches. *PLoS ONE*, *14*(5), e0215977. https://doi.org/10.1371/journal.pone.0215977

Kirwan, M. L., & Gedan, K. B. (2019). Sea-level driven land conversion and the formation of ghost forests. *Nature Climate Change*, *9*(6), 450–457. https://doi.org/10.1038/s41558-019-0488-7

Kirwan, M. L., & Guntenspergen, G. R. (2015). Response of plant productivity to experimental flooding in a stable and a submerging marsh. *Ecosystems*, *18*(5), 903–913. https://doi.org/10.1007/s10021-015-9870-0

Kirwan, M. L., Kirwan, J. L., & Copenheaver, C. A. (2007). Dynamics of an estuarine forest and its response to rising sea level. *Journal of Coastal Research*, *23*(232), 457–463. https://doi.org/10.2112/04-0211.1

Kirwan, M. L., Temmerman, S., Skeehan, E. E., Guntenspergen, G. R., & Fagherazzi, S. (2016). Overestimation of marsh vulnerability to sea level rise. *Nature Climate Change*, *6*(3), 253–260. https://doi.org/10.1038/nclimate2909

Kirwan, M. L., Walters, D. C., Reay, W. G., & Carr, J. A. (2016). Sea level driven marsh expansion in a coupled model of marsh erosion and migration. *Geophysical Research Letters*, *43*, 4366–4373. https://doi.org/10.1002/2016GL068507

Kurz, H., & Wagner, K. A. (1957). *Tidal marshes of the Gulf and Atlantic coasts of northern Florida and Charleston, South Carolina*. Tallahassee, FL: Florida State University.

Langston, A. K., Kaplan, D. A., & Putz, F. E. (2017). A casualty of climate change? Loss of freshwater forest islands on Florida's Gulf Coast. *Global Change Biology*, *23*, 5383–5397.

Mariotti, G., & Carr, J. (2014). Dual role of salt marsh retreat: Long-term loss and short-term resilience. *Water Resources Research*, *50*, 2963–2974. https://doi.org/10.1002/2013WR014676

Mccall, J. C. (2007). National data buoy center stations, 544–548. Retrieved from http://www.ndbc.noaa.gov/

McKee, K. L., & Patrick, W. H. (1988). The relationship of smooth cordgrass (*Spartina alterniflora*) to tidal datums: A review. *Estuaries*, *11*(3), 143. https://doi.org/10.2307/1351966

Morris, J., Sundareshwar, P., Nietch, C., Kjerfve, B., & Cahoon, D. (2002). Responses of coastal wetlands to rising sea level. *Ecology*, *83*(10), 2869–2877. https://doi.org/10.1890/0012-9658(2002)083[2869:ROCWTR]2.0.CO;2

Poulter, B., Qian, S. S., & Christensen, N. L. (2009). Determinants of coastal treeline and the role of abiotic and biotic interactions. *Plant Ecology*, *202*(1), 55–66. https://doi.org/10.1007/s11258-008-9465-3

Raabe, E. A., & Stumpf, R. P. (2016). Expansion of tidal marsh in response to sea-level rise: Gulf Coast of Florida, USA. *Estuaries and Coasts*, *39*(1), 145–157. https://doi.org/10.1007/s12237-015-9974-y

Robichaud, A., & Bégin, Y. (1997). The effects of storms and sea-level rise on a coastal forest margin in New Brunswick, Eastern Canada. *Journal of Coastal Research*, *13*(2), 429–439. https://doi.org/10.2307/4298638

Schieder, N. W., & Kirwan, M. L. (2019). Sea-level driven acceleration in coastal forest retreat. *Geology*, *47*(12), 1151–1155. https://doi.org/10.1130/G46607.1

Schieder, N. W., Walters, D. C., & Kirwan, M. L. (2017). Massive upland to wetland conversion compensated for historical marsh loss in Chesapeake Bay, USA. *Estuaries and Coasts*, *41*(4), 940–951. https://doi.org/10.1007/s12237-017-0336-9

Schile, L. M., Callaway, J. C., Morris, J. T., Stralberg, D., Parker, V. T., & Kelly, M. (2014). Modeling tidal marsh distribution with sea-level rise: Evaluating the role of vegetation, sediment, and upland habitat in marsh resiliency. *PLoS ONE*, *9*(2), e88760. https://doi.org/10.1371/journal.pone.0088760

Schuerch, M., Spencer, T., Temmerman, S., Kirwan, M., Wolff, C., Lincke, D., et al. (2018). Future response of global coastal wetlands to sea-level rise. *Nature*, *561*(7722), 231–234. https://doi.org/10.1038/s41586-018-0476-5

Schuerch, M., Vafeidis, A., Slawig, T., & Temmerman, S. (2013). Modeling the influence of changing storm patterns on the ability of a salt marsh to keep pace with sea level rise. *Journal of Geophysical Research: Earth Surface*, *118*, 84–96. https://doi.org/10.1029/2012JF002471

Smith, J. A. (2013). The role of *Phragmites australis* in mediating inland salt marsh migration in a mid-Atlantic estuary. *PLoS ONE*, *8*, e65091. https://doi.org/10.1371/journal.pone.0065091

Valiela, I., Teal, J. M., & Deuser, W. G. (1978). Nature of growth forms in salt-marsh grass *Spartina alterniflora*. *The American Naturalist*, *112*(985), 461–470. https://doi.org/10.1086/283290

Weinstein, M., & Kreeger, D. (Eds) (2007). *Concepts and controversies in tidal marsh ecology*. Dordrecht: Springer Netherlands.

Williams, K., Ewel, K. C., Stumpf, R. P., Putz, F. E., & Workman, T. W. (1999). Sea-level rise and coastal forest retreat on the west coast of Florida, USA. *Ecology*, *80*(6), 2045–2063. https://doi.org/10.2307/176677

Williams, K., MacDonald, M., & Lda Sternberg, S. L. (2003). Interactions of storm, drought, and sea-level rise on coastal forest: A case study. *Journal of Coastal Research*, *19*, 1116–1121.

Young, R. (1995). Coastal wetland dynamics in response to sea-level rise: transgression and erosion. (Doctoral dissertation). Durham, NC: Duke University.

References From the Supporting Information

Amateis, R. L., Burkhart, H. E., & Liu, J. (1997). Modeling survival in juvenile and mature loblolly pine plantations. *Forest Ecology and Management*, *90*(1), 51–58. https://doi.org/10.1016/S0378-1127(96)03833-9

Boon, J. D. (1975). Tidal discharge asymmetry in a salt marsh drainage system. *Limnology and Oceanography*, *20*(1), 71–80. https://doi.org/10.4319/lo.1975.20.1.0071

Carr, J. A., & Guntenspergen, G. R. (2020). Water levels (November 11 2016 through November 11 2017) for four wells and Light intensity data (October 1 2015 through September 2019): From marsh to upland forest, for Moneystump Marsh, Blackwater National Wildlife Refuge, Maryland: U.S. Geological Survey data release. https://doi.org/10.5066/P9XQ27F5

Fagherazzi, S., Hannion, M., & D'Odorico, P. (2008). Geomorphic structure of tidal hydrodynamics in salt marsh creeks. *Water Resources Research*, *44*, W02419. https://doi.org/10.1029/2007WR006289

Mariotti, G., & Fagherazzi, S. (2013). Critical width of tidal flats triggers marsh collapse in the absence of sea-level rise. *Proceedings of the National Academy of Sciences of the United States of America*, *110*(14), 5353–5356. https://doi.org/10.1073/pnas.1219600110

Mariotti, G., Kearney, W. S., & Fagherazzi, S. (2016). Soil creep in salt marshes. *Geology*, *44*(6), 459–462. https://doi.org/10.1130/G37708.1

Mudd, S. M., D'Alpaos, A., & Morris, J. T. (2010). How does vegetation affect sedimentation on tidal marshes? Investigating particle capture and hydrodynamic controls on biologically mediated sedimentation. *Journal of Geophysical Research*, *115*, F03029. https://doi.org/10.1029/2009JF001566

Schultz, R. P. (1997). Loblolly pine: The ecology and culture of loblolly pine (*Pinus taeda* L.). In *Agriculture Handbook* (Chap. 2, pp. 2-1–2-50). Washington, DC: US Department of Agriculture.

Tuttle, C. L., South, D. B., Golden, M. S., & Meldahl, R. S. (1988). Initial *Pinus taeda* seedling height relationships with early survival and growth. *Canadian Journal of Forest Research*, *18*(7), 867–871. https://doi.org/10.1139/x88-133

Whitehouse, R. J. S., Soulsby, R. L., Roberts, W., & Mitchener, H. J. (2000). *Dynamics of estuarine muds*. London, UK: Thomas Telford. https://doi.org/10.1680/doem.28647

Wilson, C. A., Hughes, Z. J., FitzGerald, D. M., Hopkinson, C. S., Valentine, V., & Kolker, A. S. (2014). Saltmarsh pool and tidal creek morphodynamics: Dynamic equilibrium of northern latitude saltmarshes? *Geomorphology*, *213*, 99–115. https://doi.org/10.1016/j.geomorph.2014.01.002